Transmission characteristics of one-dimensional periodic optical waveguide networks

Jian Zheng, Xiangbo Yang,* Xian Zhang, Dongmei Deng, and Hongzhan Liu
Guangzhou Key Laboratory for Special Fiber Photonic Devices, School of Information and Optoelectronic Science and Engineering, South China Normal University, Guangzhou 510006, China

(Received 16 October 2018; published 5 February 2019)

In this study, the transmission characteristics of one-dimensional (1D) periodic optical waveguide networks (POWNs) composed of simple or complex unit cells are systematically studied with the transfer matrix method. Using this method, the general transmission formula is analytically derived for any 1D POWNs. Due to the periodicity, three types of transmission resonance peaks can be produced, one of which shows an interesting missing order effect. The conditions for producing these phenomena are analytically obtained from the transmission formula. Moreover, it is found that transmission valleys in the passbands can be described by a simple envelope function. A greater number of waveguides in a simple unit cell or more nodes in a complex unit cell result in smaller minima of the passband transmission valley. Finally, the formula for the depth of photonic band gaps (PBGs) is analytically determined. We find that the depth of PBGs exponentially increases with the cell number and the width of PBGs becomes wider with the increase of the node in unit cells. Our work enhances people's understanding of the optical characteristics of periodic waveguide networks, and may be useful for designing all-optical devices, such as dense wavelength division multiplexers, high-efficiency optical switches, and wideband and/or narrowband optical filters.

DOI: 10.1103/PhysRevA.99.023809

I. INTRODUCTION

Photonic crystals (PhCs) are photonic band gap (PBG) structures [1,2] that can effectively confine and control the propagation of electromagnetic (EM) waves. Over the past 30 years, PhCs have received considerable research attention [1–16]. Many interesting physical phenomena, including Bloch oscillations [11] and Anderson localizations [17], have been observed in PhCs. Numerous optical devices based on PhCs have been manufactured, such as low-threshold PhC lasers [18,19], dense wavelength division multiplexers [20,21], and so on.

Optical waveguide networks [22–25], which can also confine and control the propagation of EM waves, are another type of PBG structure. However, the mechanism for generating PBGs in optical waveguide networks is different from that in PhCs. PhCs primarily depend on the periodic arrangement of dielectrics, where two or more kinds of dielectrics are needed. The difference between the dielectric constants determines the width of PBGs. On the contrary, optical waveguide networks mainly rely on the connections among waveguides, where only one dielectric is required. In this case, the width of PBGs is not closely related to the dielectric constant. Moreover, the connections of optical waveguide networks are very flexible; thus rich symmetric and high-dimensional structures can be easily implemented. Most notably, the amplitudes and phases of EM waves propagating in an optical network can be conveniently measured at the nodes. Because of its own advantages, optical networks have been widely investigated [22–33] and used as platforms for observing interesting physical phenomena, such as Anderson localizations [22,23,32], Bloch oscillations [26,27], Rabi oscillations [30], and the slow light effects [33].

However, to date, the conventional method for studying the transmission characteristics of optical waveguide networks is the generalized eigenfunction method [28], due to the diversity of unit cell structures. This method can only allow researchers to numerically calculate the transmittance and reflectance of networks. Many optical properties of networks can only be qualitatively summarized by incomplete induction based on these numerical results. Moreover, the computation load increases significantly as the unit cell number of networks increases. Therefore, it is necessary to find a more efficient method to study the optical properties of optical waveguide networks.

In this paper, based on the network equation we use a more efficient method to investigate the transmission characteristics of one-dimensional (1D) periodic optical waveguide networks (POWNs). This method is called the transfer matrix method, which is widely used in many areas such as quantum optical setups [34–36]. Using this method, a general formula for transmission is analytically obtained. On the basis of the transmission formula, three types of transmission resonance peaks are found, and the type III transmission resonance peaks which are found near the center of PBGs show an interesting missing order effect. Moreover, the conditions for producing these optical phenomena are analytically obtained. In the passbands, an envelope function describing the transmission valleys is derived. It is found that the depths of these valleys are closely related to the number of waveguide segments in a unit cell. In the stop bands, the depth of PBGs will exponentially increase with the cell number, approximately following the function of $e^{-2N\gamma}$, and the width of PBGs is closely related

*xbyang@scnu.edu.cn

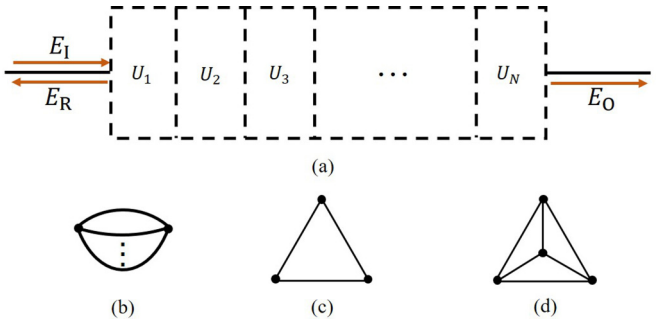

FIG. 1. Schematic diagram of 1D POWNs. (a) Overall structure of 1D POWNs, where $U_z\,(z = 1, \ldots, N)$ denotes the zth unit cell, E_I, E_R, and E_O are the incident, reflected, and transmitted EM waves, respectively, and a 1D waveguide segment of length d is connected to the entrance and the exit. (b) Multiconnected unit cell. (c) Triangular unit cell. (d) Tetrahedral unit cell.

to the unit cell structure. Compared with the generalized eigenfunction method, the transmission matrix method not only can derive the general transmission formula, but also greatly reduce the calculation load for an optical network with many cells. This work may deepen our understanding of the optical properties of periodic waveguide networks. It may be useful to design various all-optical devices, such as high-efficiency optical switches, wideband or narrowband optical filters, and so on.

This paper is organized as follows. The model of the 1D POWNs and the network equation theory are introduced in Sec. II. In Sec. III, we introduce the transfer matrix method for simple and complex unit cells and discuss the transmission properties of 1D POWNs. The conclusions of this study are drawn in Sec. IV.

II. MODEL AND NETWORK EQUATION

Figure 1(a) shows the overall structure of 1D POWNs, where $U_z\,(z = 1, \ldots, N)$ denotes the zth unit cell. Figures 1(b)–1(d) depict the three types of unit cells considered in Sec. III, and the 1D POWNs composed of these unit cells are shown in Figs. 2 and 7. In 1D POWNs, the wave function $\varphi_{ij}(x)$ within any waveguide segment between nodes i and j (black dots) satisfies the Helmholtz equation:

$$\frac{d^2\varphi_{ij}(x)}{dx^2} + \left(\frac{n\omega}{c}\right)^2 \varphi_{ij}(x) = 0, \tag{1}$$

where n is the refractive index of the waveguide segment ($n = 2$ in this study), ω is the angular frequency of the EM wave, and c is the speed of light in vacuum. According to the continuity of the wave function, the following boundary conditions

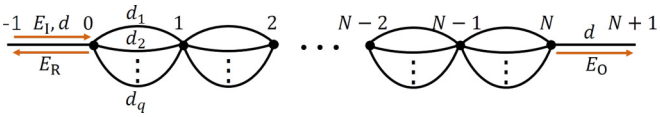

FIG. 2. Schematic diagram of 1D MPOWNs, where the lengths of the waveguide segments in each unit cell are d_1, d_2, ..., and d_q, and the lengths of the waveguide segment at the entrance and exit are d.

exist at nodes i and j: $\varphi_{ij}(x)|_{x=0} = \varphi_i$ and $\varphi_{ij}(x)|_{x=l_{ij}} = \varphi_j$, where l_{ij} represents the length of the segment between nodes i and j. With these conditions, the solution to Eq. (1) has the form [37]

$$\varphi_{ij}(x) = \varphi_i \frac{\sin[k(l_{ij} - x)]}{\sin kl_{ij}} + \varphi_j \frac{\sin kx}{\sin kl_{ij}}, \tag{2}$$

where $k = n\omega/c$. At node i, the flux conservation condition gives

$$\sum_j \left.\frac{d\varphi_{ij}(x)}{dx}\right|_{x=0} = 0. \tag{3}$$

Substituting Eq. (2) into Eq. (3), the following network equation can be obtained:

$$-\varphi_i \sum_j \cot kl_{ij} + \sum_j \csc kl_{ij}\varphi_j = 0. \tag{4}$$

III. RESULTS AND DISCUSSIONS

For simplicity, we classify the unit cells of 1D POWNs into simple and complex unit cells. A simple unit cell contains one node, whereas a complex unit cell contains two or more nodes. When the unit cells in Fig. 1 are connected into a network, adjacent cells in a network share one node. In this case, Fig. 1(b) is a simple unit cell, and Figs. 1(c) and 1(d) are complex unit cells. Next, we introduce the transfer matrix method based on Eq. (4) and use this method to investigate the transmission characteristics of 1D POWNs composed of simple or complex unit cells. These results are verified by the generalized eigenfunction method.

A. Networks composed of simple unit cells

The periodic network composed of simple unit cells is shown in Fig. 2, and this structure is called 1D multiconnected periodic optical waveguide networks (MPOWNs). The number of waveguide segments in each unit cell is q, and their lengths are d_1, d_2, ..., and d_q. For 1D MPOWNs, Eq. (4) can be rewritten as

$$\varepsilon_i\varphi_i + \kappa_{i-1,i}\varphi_{i-1} + \kappa_{i,i+1}\varphi_{i+1} = 0, \tag{5}$$

where $\varepsilon_i = -\sum_{s_{i-1,i}} \cot(kl_{i-1,i}) - \sum_{s_{i,i+1}} \cot(kl_{i,i+1})$, $\kappa_{i-1,i} = \sum_{s_{i-1,i}} \csc(kl_{i-1,i})$, and $\kappa_{i,i+1} = \sum_{s_{i,i+1}} \csc(kl_{i,i+1})$; here $s_{i-1,i}$ and $s_{i,i+1}$ represent the number of waveguide segments on either side of node i. Using Eq. (5), the recursion matrix τ_i ($i = 0, 1, \ldots, N$) can be obtained:

$$\begin{pmatrix}\varphi_{i+1}\\ \varphi_i\end{pmatrix} = \begin{pmatrix}\frac{-\varepsilon_i}{\kappa_{i,i+1}} & \frac{-\kappa_{i-1,i}}{\kappa_{i,i+1}}\\ 1 & 0\end{pmatrix}\begin{pmatrix}\varphi_i\\ \varphi_{i-1}\end{pmatrix} = \tau_i\begin{pmatrix}\varphi_i\\ \varphi_{i-1}\end{pmatrix}. \tag{6}$$

The wave functions $\varphi_{ij}(x)$ at the entrance and exit can be written as

$$\begin{aligned}\varphi_{-1,0}(x) &= e^{ik(x-d)} + r_N e^{-ik(x-d)},\\ \varphi_{N,N+1}(x) &= t_N e^{ikx},\end{aligned} \tag{7}$$

where r_N and t_N are, respectively, the reflection and transmission coefficients of networks with N unit cells. Thus transmittance and reflectance are $T_N = |t_N|^2$ and $R_N = |r_N|^2$,

respectively. From Eq. (7), we have

$$\begin{pmatrix}\varphi_0\\ \varphi_{-1}\end{pmatrix}=\begin{pmatrix}1 & 1\\ e^{-ikd} & e^{ikd}\end{pmatrix}\begin{pmatrix}1\\ r_N\end{pmatrix}=Q_L\begin{pmatrix}1\\ r_N\end{pmatrix},$$
$$\begin{pmatrix}\varphi_{N+1}\\ \varphi_N\end{pmatrix}=\begin{pmatrix}e^{ikd} & e^{-ikd}\\ 1 & 1\end{pmatrix}\begin{pmatrix}t_N\\ 0\end{pmatrix}=Q_R\begin{pmatrix}t_N\\ 0\end{pmatrix}. \quad (8)$$

Based on Eqs. (6) and (8), t_N and r_N are related through the transfer matrix M_N:

$$\begin{pmatrix}t_N\\ 0\end{pmatrix}=M_N\begin{pmatrix}1\\ r_N\end{pmatrix}=Q_R^{-1}\tau_N\tau_{N-1}\ldots\tau_1\tau_0Q_L\begin{pmatrix}1\\ r_N\end{pmatrix}. \quad (9)$$

When $N>1$,

$$\tau_{N-1}=\tau_{N-2}=\cdots=\tau_1=\tau=\begin{pmatrix}\frac{2\sum_q\cot kd_q}{\sum_q\csc kd_q} & -1\\ 1 & 0\end{pmatrix}, \quad (10)$$

and $\tau_{N-1}\tau_{N-2}\ldots\tau_1=\tau^{N-1}$. Using Chebyshev Identity [38], we can write

$$\tau^{N-1}=\frac{1}{\sin K}[\tau\ \sin(N-1)K-I\ \sin(N-2)K], \quad (11)$$

where I is an identity matrix and K is the magnitude of the generalized Bloch wave vector $\mathbf{K}$ [29]. Substituting Eq. (11) into Eq. (9), we obtain

$$M_N=\frac{1}{\sin K}[M_2\sin(N-1)K-M_1\sin(N-2)K]. \quad (12)$$

Moreover, t_N, r_N, and the elements of M_N satisfy the following relations:

$$r_N=-\frac{(M_N)_{21}}{(M_N)_{22}},$$
$$t_N=\frac{1}{(M_N)_{22}},$$
$$\frac{r_N}{t_N}=-(M_N)_{21}. \quad (13)$$

Further, the relationship between the trace of τ and K satisfies

$$\mathrm{Tr}\,\tau=2\cos K. \quad (14)$$

Using Eqs. (13) and (14), we obtain that $(r_2/t_2)/(r_1/t_1)=\mathrm{Tr}\,\tau=2\cos K$. Then, from Eqs. (12) and (13), we can show

$$\frac{r_N}{t_N}=\frac{r_1}{t_1}\frac{\sin NK}{\sin K}. \quad (15)$$

Finally, by means of Eq. (15) and $T+R=1$, the general transmission formula for 1D MPOWNs is derived as follows:

$$T_1=\left|\frac{1}{(M_1)_{22}}\right|^2,$$
$$T_N=\left[1+\left(\frac{1}{T_1}-1\right)\left(\frac{\sin NK}{\sin K}\right)^2\right]^{-1}. \quad (16)$$

In the following subsections, Eq. (16) is used to analytically investigate the transmission properties of 1D MPOWNs.

1. Networks with q = 2

In Fig. 2, a simple unit cell with two waveguide segments (i.e., $q=2$) forms the simplest simple unit cell, and

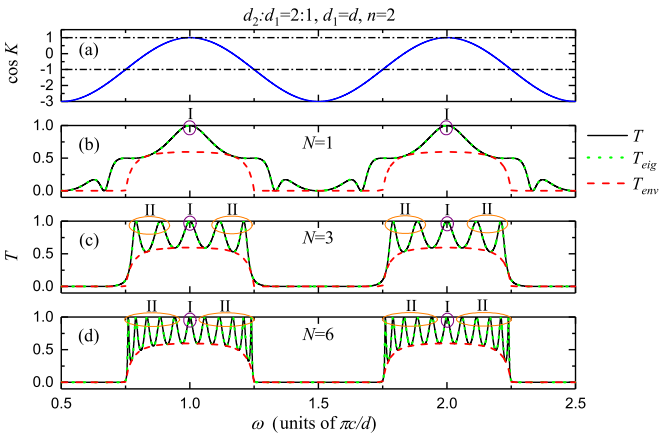

FIG. 3. Dispersion and transmission spectra of 1D MPOWNs with $d_2:d_1=2:1$ and $d_1=d$. (a) Dispersion spectrum. Transmission spectra for the network containing (b) one, (c) three, and (d) six unit cells, where the black solid lines are obtained by the transfer matrix method [i.e., Eq. (16)], the green (gray) dotted lines are obtained by the generalized eigenfunction method, and the red (gray) dashed lines are the envelope curves of the passband transmission valleys determined by Eq. (21).

optical waveguide networks with $d_2:d_1=2:1$ and $d_1=d$ are known to produce large PBGs [29,31]. Therefore, we first investigate the transmission properties of 1D MPOWNs composed of the simplest simple unit cell. By means of Eqs. (6)–(9), the transfer matrix M_1 for the network with one cell is

$$M_1=Q_R^{-1}\begin{pmatrix}\frac{9\cos^2 2\theta+\cos 2\theta-2}{2\cos 2\theta+1} & -\frac{3\cos 2\theta+2}{2\cos\theta+1}\\ \frac{3\cos 2\theta+2}{2\cos\theta+1} & \frac{-2\cos\theta}{2\cos\theta+1}\end{pmatrix}Q_L, \quad (17)$$

where $\theta=kd$. For this kind of network, Eq. (10) can be simplified to

$$\tau=\begin{pmatrix}4\cos\theta-2 & -1\\ 1 & 0\end{pmatrix}, \quad (18)$$

and the dispersion function can be obtained using Eqs. (14) and (18):

$$\cos K=2\cos kd-1. \quad (19)$$

In Fig. 3, Eqs. (16), (17), and (19) are used to plot the dispersion and transmission spectra of 1D MPOWNs. Transmission spectra calculated by the generalized eigenfunction method are also shown in Fig. 3. From Figs. 3(b)–3(d), we observe that the results calculated by the transfer matrix method (black solid line) are identical with those obtained by the generalized eigenfunction method [green (gray) dotted line].

Type I transmission resonance peak. From Eq. (16), when $T_1=1$, $T_N=1$. Transmission peaks with $T_1=1$ will appear in the 1D MPOWN transmission spectrum. We refer to this peak as the type I transmission resonance peak. In Figs. 3(b)–3(d), the peaks at $\pi c/d$ and $2\pi c/d$ are the type I transmission resonance peak and are labeled as "I". In general, for 1D MPOWNs with $d_2:d_1=2:1$ and $d_1=d$, such peaks are located at $\omega_{\mathrm{I}}=\alpha\pi c/d$, where α is an integer. Since the condition for generating type I peak is $T_1=1$, the unit cell is a completely transparent unit cell at $T_1=1$, and a network

composed of one or more transparent unit cells is also transparent.

Type II transmission resonance peak. From Eq. (16), when $\sin NK = 0$ and $\sin K \neq 0$ (i.e., $NK = m\pi$, $m = 1, 2, \ldots, N-1$), $T_N \equiv 1$ ($N > 1$). It means that the transmission spectrum of a network with N cells will form another $N-1$ transmission resonance peak due to the periodicity. We refer to these peaks as the type II transmission resonance peak. According to Eq. (19), these peaks will appear at frequency

$$\omega_{\mathrm{II}} = \frac{c}{nd} \arccos\left(\frac{1}{2}\cos\frac{m\pi}{N} + \frac{1}{2}\right). \tag{20}$$

As shown in Fig. 3, the transmission spectrum for one cell [Fig. 3(b)] cannot generate the type II transmission resonance peak. However, when $N > 1$, there exist $N-1$ transmission resonance peaks in every monotonic interval of the dispersive function. These peaks are labeled as "II". From Eq. (20), these type II transmission resonance peaks in Fig. 3(c) are located at $0.790215\pi c/d$, $0.884973\pi c/d$, $1.115027\pi c/d$, $1.209785\pi c/d$, $1.790215\pi c/d$, $1.884973\pi c/d$, $2.115027\pi c/d$, and $2.209785\pi c/d$. Similarly, the frequency of the type II transmission resonance peak in Fig. 3(d) can also be obtained by using Eq. (20). All these transmission resonances are Bragg resonances, which are attributed to the increase of cell number.

Envelope function of passband transmission valleys. In the passbands, $|\cos NK| \leqslant 1$, K is a real number. From Eq. (16), the transmittance at any frequency will oscillate with the cell number N in this region. Thus the transmission valleys in the passbands may appear at different frequencies for a network with different cell number. If we set $|\sin NK| = 1$, the envelope function of the passband transmission valleys can be obtained:

$$T_{\mathrm{env}} = \left[1 + \left(\frac{1}{T_1} - 1\right)\frac{1}{\sin^2 K}\right]^{-1}. \tag{21}$$

The envelope function is visibly independent of the cell number. Hence any transmission valleys in the passbands should satisfy this envelope function. The red (gray) dashed lines in Figs. 3(b)–3(d) represent the envelope curve of the passband transmission valleys described by Eq. (21). The envelope function describes the minimum transmittance at any frequency in the passbands.

Depth of PBGs. In the stop bands, $|\cos K| > 1$, K is $\pi + i\gamma$ or $i\gamma$, where γ is a real number. From Eq. (16), the depths of PBGs of 1D MPOWNs with N cells is given by

$$T_N \approx e^{-2N\gamma}\left(\frac{1}{T_1} - 1\right)^{-1}. \tag{22}$$

The depth of the PBGs clearly increases exponentially with the cell number N, approximately following the function of $e^{-2N\gamma}$. This is a typical feature of the difference between the stop band and the passband. The transmission spectra of 1D OMRPOWNs containing two, five, and ten cells is shown in Fig. 4. As the number of unit cells increases, the PBGs exponentially deepen.

Type III transmission resonance peak. In the above analysis, we have investigated the transmission properties of 1D MPOWNs with $d_2 : d_1 = 2 : 1$. Now, we investigate the

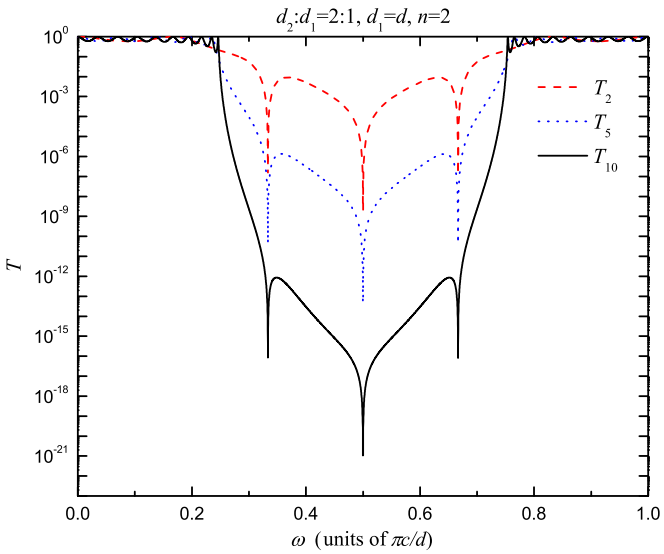

FIG. 4. Transmission spectra of 1D MPOWNs with $d_2 : d_1 = 2 : 1$, where red (gray) dashed line, blue (gray) dotted line, and black solid line are, respectively, the results of the networks with $N = 2$, 5, and 10.

transmission properties of 1D MPOWNs with $d_2 : d_1 = 1.99 : 1$. In this case, the dispersion function changes from Eq. (19) to

$$\cos K = \frac{\cot kd + \cot 1.99kd}{\csc kd + \csc 1.99kd}. \tag{23}$$

The dispersion and transmission spectra of 1D MPOWNs with $d_2 : d_1 = 1.99 : 1$ are plotted in Fig. 5, where Figs. 5(e)–5(h) are enlarged views of Figs. 5(a)–5(d), respectively. Comparing Fig. 5 with Fig. 3, several ultranarrow transmission peaks are produced near the center of the stop band. These peaks are referred to as the type III transmission resonance peak. From Figs. 5(a) and 5(e), in the frequency range $1.49\pi c/d$–$1.52\pi c/d$, the dispersion function $\cos K$ forms a sharp peak passing through stop band

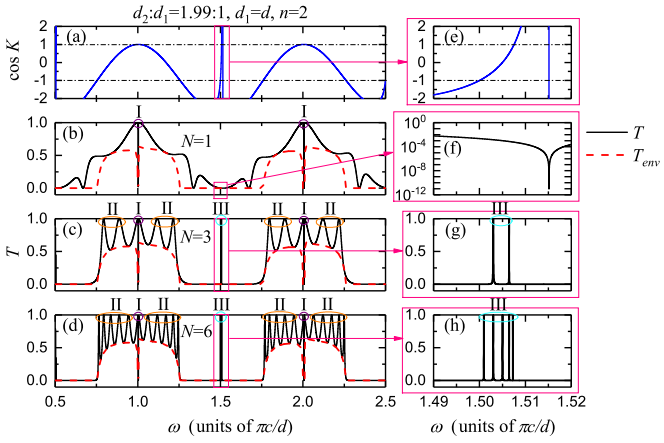

FIG. 5. Dispersion and transmission spectra of 1D MPOWNs with $d_2 : d_1 = 1.99 : 1$. (a) Dispersion spectrum. Transmission spectra with (b) one, (c) three, and (d) six unit cells. Panels (e)–(h) are the enlarged versions of (a)–(d), respectively. The black solid lines are transmission curves and the red (gray) dashed lines are the envelope curves of the passband transmission valley.

→ passband → stop band → passband → stop band, successively, and in turn, K is a complex number → real number → complex number → real number → complex number. In the passband between frequency $1.50\pi c/d$ and $1.51\pi c/d$, $5\times10^{-4} < T_1 < 2.25\times10^{-3}$. When $\sin NK$ tends to zero, $\sin NK \to 0$ is a higher order of infinitesimal to T_1. Consequently, when $\sin NK$ tends to zero, $\sin^2 NK/T_1$ goes to zero. For convenience, Eq. (16) is rewritten as follows:

$$T_N = \left[1 + \left(\frac{\sin^2 NK}{T_1} - \sin^2 NK\right)\frac{1}{\sin^2 K}\right]^{-1}. \tag{24}$$

From this equation, T_N tends to be one when $\sin^2 NK/T_1 \to 0$ in the frequency range of $1.50\pi c/d$–$1.51\pi c/d$. Thus the $N-1$ type III transmission resonance peaks can form in the narrow passband area. It indicates that Bragg resonance can still form because of the periodicity in the narrow passband. From Fig. 5(g), when the cell number is three (i.e., $N=3$), two total transparent transmission peaks of type III at frequencies of $1.503007\pi c/d$ and $1.506458\pi c/d$ are obtained, and we label them as III. Similarly, when the number of cells is six (i.e., $N=6$), as shown in Figs. 5(d) and 5(h), there are five total transparent transmission peaks. Based on the above analysis, when the waveguide length ratio is $d_2 : d_1 = 1.99 : 1$, the conditions for the type III transmission resonance peak are $\sin Nk \to 0$ and $\sin^2 NK/T_1 \to 0$.

Missing order effect of type III transmission resonance peak. Based on Eqs. (17) and (23), and Figs. 5(e) and 5(f), T_1 is a higher-order infinitesimal than $\sin^2 Nk \to 0$ when the frequency approaches $1.515\pi c/d$. Thus $\sin^2 NK/T_1 \to \infty$ near $1.515\pi c/d$. From Eq. (24), T_N goes to zero in this case. In other words, although K is a real number in this ultranarrow area, it is difficult to form Bragg resonance for the network. We refer to this phenomenon as the missing order effect of the type III transmission resonance peak. In Figs. 5(b)–5(d) and 5(f)–5(h), there does not exist any transmission resonance peak near $1.515\pi c/d$. Briefly, when the waveguide length ratio is $d_2 : d_1 = 1.99 : 1$, the conditions for missing order effect are $\sin Nk \to 0$, and $\sin^2 NK/T_1 \to \infty$.

2. Networks with q > 2

From Fig. 2, for most simple unit cells, q is greater than two. In this subsection, the transmission properties of 1D MPOWNs with $q > 2$ are investigated. When the cell number is $N = 1$, the transfer matrix M_1 can be deduced as follows:

$$M_1 = Q_R^{-1}\begin{pmatrix} \frac{A-B^2\sin\theta+\sin\theta\,\cos^2\theta}{B} & -\frac{A+\cos\theta}{B} \\ \frac{A+\cos\theta}{B} & -\frac{\csc\theta}{B} \end{pmatrix} Q_L, \tag{25}$$

where $A = \sum_q \cot\theta_q$, $B = \sum_q \csc\theta_q$, $\theta = kd$, and $\theta_q = kd_q$. When $N > 1$, the dispersive function can be derived from Eqs. (10) and (14):

$$\cos K = \frac{\sum_q \cot kd_q}{\sum_q \csc kd_q}. \tag{26}$$

The transmittance T_N of 1D MPOWNs with $q > 2$ can be calculated by use of Eqs. (16) and (25). Therefore, the envelope curve of passband transmission valleys for networks with $q > 2$ can also be described by Eq. (21). Furthermore, the three types of transmission resonance peaks and the missing order effect can also be produced by these networks with $q > 2$ on the same conditions. In the stop bands, the depth of the PBGs still increases exponentially with the cell number N.

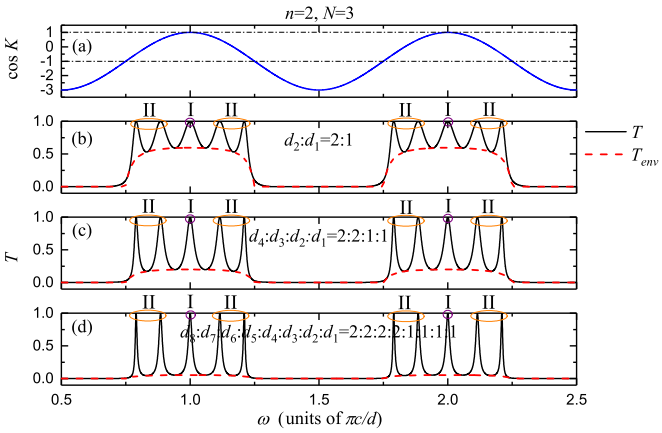

FIG. 6. Dispersion and transmission spectra of 1D MPOWNs. (a) Dispersion spectrum. Transmission spectra for 1D MPOWNs with (b) $d_2 : d_1 = 2 : 1$, (c) $d_4 : d_3 : d_2 : d_1 = 2 : 2 : 1 : 1$, and (d) $d_8 : d_7 : \ldots : d_2 : d_1 = 2 : 2 : 2 : 2 : 1 : 1 : 1 : 1$. The black solid lines are the transmission curves and the red (gray) dashed lines are the envelope curves of the passband transmission valley.

To directly analyze the influence of the number of waveguide segments in a unit cell on transmission characteristics, we investigate the transmission properties of three kinds of networks with $q = 2, 4, 8$, and set the waveguide length ratios as $d_2 : d_1 = 2 : 1$, $d_4 : d_3 : d_2 : d_1 = 2 : 2 : 1 : 1$, and $d_8 : d_7 : \ldots : d_2 : d_1 = 2 : 2 : 2 : 2 : 1 : 1 : 1 : 1$, respectively. Using Eqs. (16), (25), and (26), the dispersion and transmission spectra for 1D MPOWNs with three unit cells are presented in Fig. 6. Comparison of Figs. 6(c) and 6(d) with Fig. 6(b) shows that 1D MPOWNs with $q > 2$ can also produce the same type of transmission resonance peak, and their number and frequency positions are the same as those of 1D MPOWNs with $q = 2$. It is noticeable that valleys in the passbands become deeper as the number of waveguide segments increases. This phenomenon is due to the fact that the scattering effect of EM waves is enhanced as the number of waveguide segment increases.

B. Networks composed of complex unit cells

In this section, the transfer matrix method for any complex unit cell is introduced in detail, and we use this method to investigate the transmission characteristics of 1D POWNs composed of complex unit cells. Schematic diagrams of 1D POWNs composed of triangular or tetrahedral unit cells are shown in Fig. 7. In 1D POWNs, a triangular unit cell possesses two nodes, whereas a tetrahedral unit cell possesses three nodes.

1. General transmission formula

A complex unit cell contains two or more nodes. We divide the nodes in a complex unit cell into two categories: internal and boundary nodes. For example, nodes $1, 3, \ldots, 2N-1$ in Fig. 7(a) and nodes $1, 2, 4, 5, \ldots, 3N-2, 3N-1$ in

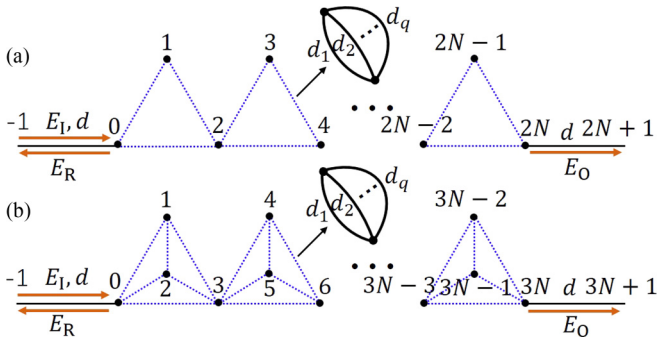

FIG. 7. 1D POWNs composed of complex cells. (a) 1D triangular periodic optical waveguide networks. (b) 1D tetrahedral periodic optical waveguide networks.

Fig. 7(b) are internal nodes, whereas nodes $0, 2, 4, \ldots, 2N$ in Fig. 7(a) and nodes $0, 3, 6, \ldots, 3N$ in Fig. 7(b) are boundary nodes. If the total number of nodes in each unit cell is w, the number of internal nodes is $w-1$. For the ith internal node of the zth unit cell in Fig. 7, Eq. (4) can be rewritten as

$$w\varepsilon\varphi_i + \kappa \sum_{p=w(z-1)+1}^{wz-1} \varphi_p + \kappa(\varphi_{w(z-1)} + \varphi_{wz}) = 0, \tag{27}$$

where $\varepsilon = -\sum_q \cot kd_q$, $\kappa = \sum_q \csc kd_q$, $p \neq i$, and $z \geqslant 1$. For the boundary nodes of the zth unit cell, Eq. (4) can be rewritten as

$$2w\varepsilon\varphi_{w(z-1)} + \kappa(\varphi_{wz} + \varphi_{w(z-2)}) + \kappa \sum_{p=w(z-2)+1}^{wz-1} \varphi_p = 0, \tag{28}$$

where $p \neq w(z-1)$ and $z \geqslant 2$. From Eqs. (27) and (28), we can deduce

$$\varphi_{w(z-1)}\left[2w\varepsilon - \frac{2(w-1)\kappa^2}{(w-2)\kappa + w\varepsilon}\right] + (\varphi_{wz} + \varphi_{w(z-2)})\left[\kappa - \frac{(w-1)\kappa^2}{(w-2)\kappa + w\varepsilon}\right] = 0. \tag{29}$$

Then, the following recursive relation can be obtained according to Eq. (29):

$$\begin{pmatrix} \varphi_{wz} \\ \varphi_{w(z-1)} \end{pmatrix} = \begin{pmatrix} 2 - \frac{2w(\varepsilon+\kappa)}{\kappa} & -1 \\ 1 & 0 \end{pmatrix} \begin{pmatrix} \varphi_{w(z-1)} \\ \varphi_{w(z-2)} \end{pmatrix} = \tau_{w(z-1)} \begin{pmatrix} \varphi_{w(z-1)} \\ \varphi_{w(z-2)} \end{pmatrix}, \tag{30}$$

where the recursive matrix $\tau_{w(z-1)}$ satisfies

$$\mathrm{Tr}\, \tau_{w(N-1)} = 2\cos K. \tag{31}$$

For nodes zero and wN connecting the entrance and exit, Eq. (4) can be rewritten as

$$\varphi_0(w\varepsilon - \cot kd) + \varphi_{-1}\csc kd + \kappa\sum_{i=1}^{w}\varphi_i = 0,$$
$$\varphi_{wN}(w\varepsilon - \cot kd) + \kappa \sum_{wN-1}^{i=w(N-1)} \varphi_i + \varphi_{wN+1}\csc kd = 0. \tag{32}$$

Using Eqs. (27) and (32), we have

$$\tau_0 = \begin{pmatrix} \frac{(w-1)\kappa^2 - w^2\varepsilon^2 + (2-w-2w\varepsilon+w^2\varepsilon)\kappa + w\varepsilon\cot kd}{\kappa(\kappa-\omega\varepsilon)} & \frac{[(w-2)\kappa+w\varepsilon]\csc kd}{\kappa(\kappa-\omega\varepsilon)} \\ 1 & 0 \end{pmatrix},$$
$$\tau_{wN} = \begin{pmatrix} \cos kd + \frac{(\kappa-w\varepsilon)(\kappa w-\kappa+w\varepsilon)\sin kd}{(w-2)\kappa+w\varepsilon} & \frac{\kappa(\kappa-w\varepsilon)\sin kd}{(w-2)\kappa+w\varepsilon} \\ 1 & 0 \end{pmatrix}. \tag{33}$$

Combining Eqs. (8), (30), and (33), we find that the transmission coefficient t_N, reflection coefficient r_N, and transfer matrix M_N of 1D POWNs composed of complex unit cells satisfy the following relation:

$$\begin{pmatrix} t_N \\ 0 \end{pmatrix} = M_N \begin{pmatrix} 1 \\ r_N \end{pmatrix} = Q_R^{-1}\tau_{wN}\tau_{w(N-1)}\ldots\tau_w\tau_0 Q_L \begin{pmatrix} 1 \\ r_N \end{pmatrix}. \tag{34}$$

Obviously, the transfer matrix M_N in Eq. (34) can also be expressed as Eq. (12). Consequently, the transmittance T_N still satisfies Eq. (16), where T_1 and K are different for different unit cell structures.

2. *Networks with* $w = 2, 3$

For 1D POWNs composed of triangular and tetrahedral unit cells, the dispersion functions can be deduced by Eqs. (30) and (31):

$$\cos K_{\mathrm{Tri}} = -\frac{2\varepsilon+\kappa}{\kappa},$$
$$\cos K_{\mathrm{Tet}} = -\frac{3\varepsilon+2\kappa}{\kappa}. \tag{35}$$

As an example, the number of waveguide segment q between adjacent nodes is set to two, and the waveguide length ratio is set to $d_2 : d_1 = 2 : 1$ and $d_1 = d$. In Figs. 8 and 9, we plot the dispersion and transmission spectra of these two networks by using Eqs. (16), (34), and (35). In

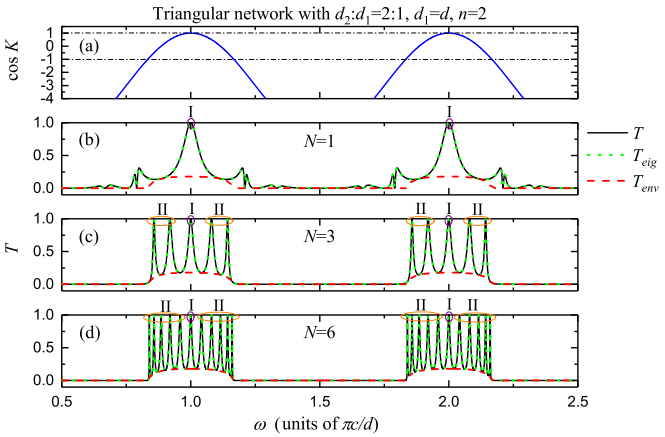

FIG. 8. Dispersion and transmission spectra of 1D triangular periodic optical waveguide networks. (a) Dispersion spectrum. Transmission spectra of the network with (b) one, (c) three, and (d) six triangular unit cells, where the black solid lines are the results calculated by the transfer matrix method [i.e., Eq. (16)], the green (gray) dotted lines are the results obtained by the generalized eigenfunction method, and the red (gray) dashed lines are the envelope curves of the transmission valley in passband.

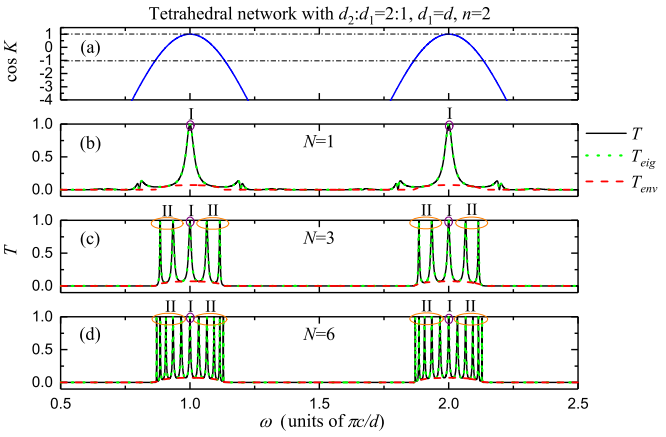

FIG. 9. Dispersion and transmission spectra of 1D tetrahedral periodic optical waveguide networks. (a) Dispersion spectrum. Transmission spectra for the network with (b) one, (c) three, and (d) six tetrahedral unit cells, where the black solid lines are the results calculated by the transfer matrix method [i.e., Eq. (16)], the green (gray) dotted lines are the results obtained by the generalized eigenfunction method, and the red (gray) dashed lines are the envelope curves of the transmission valley in passband.

order to verify the correctness of the transfer matrix method for complex cells, we also use the generalized eigenfunction method to calculate the transmittance of these two networks. From Figs. 8 and 9, we observe that the results obtained by these two methods are the same. It demonstrates that the transfer matrix method introduced by us is completely correct.

Since the transmittance T_N of 1D POWNs composed of complex unit cells still satisfies Eq. (16), the transmission properties of these two networks are similar to those of 1D POWNs composed of simple unit cells. As can be seen from Figs. 3, 8, and 9, their transmission characteristics are similar to each other. Moreover, from Figs. 3, 8, and 9, we observe that, as the number of nodes in a unit cell increases, the width of passbands will become narrow and the depth of the transmission valleys in passbands will deepen. These phenomena indicate that the scattering effect of a network composed of complex cells is much stronger than that of a network composed of simple cells.

In this section, we introduce a transfer matrix method, which is suitable for any complex unit cells. This method will help us to investigate the optical properties of waveguide networks. Based on this method, we find that, for any 1D periodic network, their transmission characteristics can be described by a general transmission formula.

IV. CONCLUSION

In this study, we investigate the transmission characteristics of 1D POWNs composed of simple or complex unit cells by use of the transfer matrix method, which is based on the network equation, and the results are verified using the generalized eigenfunction method. For 1D POWNs composed of simple unit cells, the general transmission formula is analytically obtained by use of the transfer method. On the basis of the transmission formula, three types of transmission resonance peaks are found, and the conditions for producing these resonance peaks are analytically deduced. Moreover, we find the missing order effect of the type III transmission resonance peak near the center of PBGs. Furthermore, for these transmission valleys in the passbands, an envelope function independent of the cell number is analytically derived, and the depths of these valleys increase with the number of waveguide segments in a unit cell. Finally, an approximate function describing the relationship between the depth of PBGs and the cell number is obtained. This function indicates that the depth of PBGs increases with the cell number, approximately following $e^{-2N\gamma}$. For complex unit cells, the transfer matrix is very difficult to derive. We introduce the transfer matrix method suitable for an arbitrary complex unit cell in detail. It is found that the general transmission formula is suitable for any periodic 1D networks. Thus the transmission characteristic of 1D POWNs composed of complex unit cells is similar to those introduced above. Moreover, it is found that the more complex the cell structure is, the wider the stop bands will be. These results may be useful for designing all-optical devices, such as high-efficiency optical switches, ultranarrow optical filters, and dense wavelength division multiplexers.

ACKNOWLEDGMENTS

This work was supported by the National Natural Science Foundation of China, Grants No. 11674107, No. 61475049, No. 11775083, No. 61875057, No. 61774062, and No. 61771205, and the Natural Science Foundation of Guangdong Province, Grant No. 2015A030313374.

[1] E. Yablonovitch, Phys. Rev. Lett. **58**, 2059 (1987).
[2] S. John, Phys. Rev. Lett. **58**, 2486 (1987).
[3] E. Yablonovitch, T. J. Gmitter, R. D. Meade, A. M. Rappe, K. D. Brommer, and J. D. Joannopoulos, Phys. Rev. Lett. **67**, 3380 (1991).
[4] T. F. Krauss, R. M. D. L. Rue, and S. Brand, Nature (London) **383**, 699 (1996).
[5] M. C. Wanke, O. Lehmann, K. Müller, Q. Wen, and M. Stuke, Science **275**, 1284 (1997).
[6] M. Maldovan and E. L. Thomas, Nat. Mater. **3**, 593 (2004).
[7] K. Nozaki, T. Tanabe, A. Shinya, S. Matsuo, T. Sato, H. Taniyama, and M. Notomi, Nat. Photon. **4**, 477 (2010).
[8] R. Beravat, G. K. L. Wong, M. H. Frosz, M. X. Xiao, and P. S. J. Russell, Sci. Adv. **2**, e1601421 (2016).
[9] Z. Zhang and S. Satpathy, Phys. Rev. Lett. **65**, 2650 (1990).
[10] J. B. Pendry and A. MacKinnon, Phys. Rev. Lett. **69**, 2772 (1992).
[11] M. B. Dahan, E. Peik, J. Reichel, Y. Castin, and C. Salomon, Phys. Rev. Lett. **76**, 4508 (1996).
[12] S. Fan, P. R. Villeneuve, J. D. Joannopoulos, and E. F. Schubert, Phys. Rev. Lett. **78**, 3294 (1997).
[13] Z. Wang, J. Wu, X. Liu, Y. Zhu, and N. Ming, Phys. Rev. B **56**, 9185 (1997).
[14] J. Shin and S. Fan, Opt. Lett. **30**, 2397 (2005).
[15] H. Gersen, T. J. Karle, R. J. P. Engelen, W. Bogaerts, J. P. Korterik, N. F. van Hulst, T. F. Krauss, and L. Kuipers, Phys. Rev. Lett. **94**, 073903 (2005).
[16] Y. Liu, F. Qin, Z. M. Meng, F. Zhou, Q. H. Mao, and Z. Y. Li, Opt. Express **19**, 1945 (2011).
[17] P. W. Anderson, Rev. Mod. Phys. **50**, 191 (1978).
[18] K. Sakoda, K. Ohtaka, and T. Ueta, Opt. Express **4**, 481 (1999).
[19] P. H. Weng, T. T. Wu, T. C. Lu, and S. C. Wang, Opt. Lett. **36**, 1908 (2011).
[20] A. D'Orazio, M. D. Sario, V. Petruzzelli, and F. Prudenzano, Opt. Express **11**, 230 (2003).
[21] R. Ryf, S. Randel, A. H. Gnauck, C. Bolle, A. Sierra, S. Mumtaz, M. Esmaeelpour, E. C. Burrows, R. J. Essiambre, and P. J. Winzer, J. Lightw. Technol. **30**, 521 (2012).
[22] L. Dobrzynski, A. Akjouj, B. Djafari-Rouhani, J. O. Vasseur, and J. Zemmouri, Phys. Rev. B **57**, R9388 (1998).
[23] Z. Q. Zhang, C. C. Wong, K. K. Fung, Y. L. Ho, W. L. Chan, S. C. Kan, T. L. Chan, and N. Cheung, Phys. Rev. Lett. **81**, 5540 (1998).
[24] J. O. Vasseur, B. Djafari-Rouhani, L. Dobrzynski, A. Akjouj, and J. Zemmouri, Phys. Rev. B **59**, 13446 (1999).
[25] S. K. Cheung, T. L. Chan, Z. Q. Zhang, and C. T. Chan, Phys. Rev. B **70**, 125104 (2004).
[26] T. Pertsch, P. Dannberg, W. Elflein, A. Bräuer, and F. Lederer, Phys. Rev. Lett. **83**, 4752 (1999).
[27] R. Morandotti, U. Peschel, J. S. Aitchison, H. S. Eisenberg, and Y. Silberberg, Phys. Rev. Lett. **83**, 4756 (1999).
[28] M. Li, Y. Liu, and Z. Q. Zhang, Phys. Rev. B **61**, 16193 (2000).
[29] Z. Y. Wang and X. Yang, Phys. Rev. B **76**, 235104 (2007).
[30] K. Shandarova, C. E. Ruter, D. Kip, K. G. Makris, D. N. Christodoulides, O. Peleg, and M. Segev, Phys. Rev. Lett. **102**, 123905 (2009).
[31] Q. Xiao, X. Yang, J. Lu, and C. Liu, Opt. Commun. **285**, 3775 (2012).
[32] B. Pal, P. Patra, J. P. Saha, and A. Chakrabarti, Phys. Rev. A **87**, 023814 (2013).
[33] A. Nandy and A. Chakrabarti, Phys. Rev. A **93**, 013807 (2016).
[34] J. T. Shen and S. Fan, Opt. Lett. **30**, 2001 (2005).
[35] A. Asenjo-Garcia, M. Moreno-Cardoner, A. Albrecht, H. J. Kimble, and D. E. Chang, Phys. Rev. X **7**, 031024 (2017).
[36] I. M. Mirza, J. G. Hoskins, and J. C. Schotland, Phys. Rev. A **96**, 053804 (2017).
[37] Z. Q. Zhang and P. Sheng, Phys. Rev. B **49**, 83 (1994).
[38] P. Yeh, A. Yariv, and C. S. Hong, J. Opt. Soc. Am. **67**, 423 (1977).